

FOCUSED HIGH FREQUENCY ULTRASONIC TRANSDUCERS FOR MINIMALLY INVASIVE IMAGING

Aaron Fleischman, Rushabh Modi, Anuja Nair, Geoffrey Lockwood, Shuvo Roy
Department of Biomedical Engineering, The Cleveland Clinic Foundation
9500 Euclid Avenue, Cleveland, Ohio 44195

ABSTRACT

Spherically focused, high frequency (30-50 MHz) ultrasonic imaging transducers are fabricated by using a piezoelectric polymer film and membrane deflection technique that is compatible with CMOS circuit fabrication. Micromachined ultrasonic transducers with 0.5-2.0 mm-diameter apertures and f-numbers ranging from 1.3-4.0 are fabricated and characterized. The transducers exhibit focused radiation patterns with 50 μm axial resolution and bandwidths of 80-100% around center frequency values. Tissue imaging capabilities of the micromachined ultrasonic transducers are demonstrated through successful imaging of human cadaveric aorta.

INTRODUCTION

Minimally invasive medical procedures (such as balloon angioplasty) are becoming increasingly popular to treat a variety of diseases. In some cases, minimally invasive procedures are the only therapeutic option as conventional approaches may cause irreparable harm to the patient. In cases where conventional surgical approaches exist, minimally invasive procedures provide many advantages, including reduced post-operative pain, shorter hospital stays, faster healing, and reduced scarring. A significant disadvantage for the surgeon performing a minimally invasive procedure is the lack of the direct sensory feedback, of touch-and-feel as well as visualization that the conventional approaches allow. High frequency (30–100 MHz) ultrasonic imaging technology is an approach that can be used to overcome some of these limitations, as it can provide microscopic resolution of surface and subsurface tissue structures as well as identification of physiological landmarks. Minimally invasive procedures used to treat coronary artery disease have used intravascular ultrasound (IVUS) images (30–45 MHz) for general navigation and differentiation of diseased and healthy tissue as well as deployment and placement evaluation of intracoronary stents [1, 2].

A primary limitation in conventional ultrasonic imaging technology for minimally invasive procedures is the relatively poor image quality provided by current unfocused transducers. These devices are usually slivers of lead zirconium titanate (PZT) that are chipped manually from large pieces of PZT. Consequently, there are wide variances in performance between transducers, and hence, catheter images. The unfocused nature of the transducers result in poor lateral resolution and reduced

sound intensity in the imaging volume, which limits signal-to-noise-ratio (SNR). This paper describes the fabrication and characterization of micromachined high frequency (30-50 MHz) focused polymer ultrasonic transducers that can be integrated with electronics and can be miniaturized to $<1\text{mm}^3$ for catheter mounting.

POLYMER TRANSDUCERS

Polymer-based piezoelectric materials such as polyvinylidene difluoride (PVDF) and its copolymers can enable high frequency, large bandwidth, ultrasonic transducers and can be readily shaped into spherically focused radiators for high resolution images [3, 4]. However, small polymer transducers usually require a high impedance preamplifier in close physical proximity to reduce signal degradation in the cable [5]. Previous work in the development of ultrasonic transducers include: integration of polymer ultrasonic transducers with electronics [6, 7]; micromachined Si to improve transducer performance [8]; and dome shaped micromachined Si diaphragms for transducers [9]. This paper demonstrates the successful operation of mechanically focused miniature high frequency ultrasonic transducers created using micromachining techniques that are IC compatible and scalable to create transducers of arbitrary aperture and focus.

DEVICE FABRICATION

Cross-sectional and plan schematic views of the transducer are shown in Figure 1. The plan view depicts the concept for integrating the transducer with electronics,

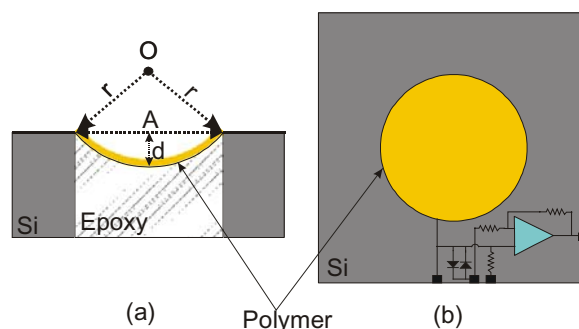


Figure 1. (a) Cross-sectional view of spherically focused ultrasonic transducer showing pertinent geometry. (b) Plan view depicting the approach for integrating a preamplifier with the transducer.

while the cross-sectional view shows the critical geometries of the deformed polymer membrane. The f-number of the device is defined to be r/A , where r is the radius of curvature and A is the diameter of the aperture. The focal point of transducer is at point O . From the geometry, it is apparent that changing the center of deflection for a given aperture is sufficient to change the radius of curvature of the deformed membrane, which then changes the f-number. Circular polymer membranes with clamped boundaries deform spherically under uniformly applied differential pressure. The center deflection is a function of membrane geometry, materials properties, and differential pressure, and is described by [10]:

$$P = \frac{C_1}{a^2} \sigma_o d + \frac{C_2 f(v) t}{a^4} \frac{E}{1-\nu} d^3 \quad (1)$$

where P is differential pressure, a is radius of the membrane ($A/2$), E is the Young's modulus, ν is the Poisson ratio, σ_o is the residual stress, d is the center deflection, $f(v)$ is a dimensionless function, t is the membrane thickness, and C_1 and C_2 are geometrically dependant constants. Thus, the f-number for arbitrarily sized apertures can be controlled by change in air pressure.

Freestanding 9 μm -thick PVDF films with 200 nm-thick gold coating on one side are used as the piezoelectric polymer material. Laser micromachining is used to form 0.5-2.0 mm-diameter apertures in a Si wafer, which is subsequently oxidized thermally to grow a 1.5 μm -thick oxide. The wafer is then diced into 1 cm-wide square die to create the substrates for the transducers. Alternatively, transducers can be fabricated using spun-on PVDF-TrFe (a PVDF copolymer) films [7] and deep reactive ion etching (DRIE). The die with the suspended polymer film is inverted onto a jig and pressure is used to deform the film as shown in Figure 2. Afterwards, a conductive epoxy is placed in the hole to act as the backside contact and sound absorbing backing as well as fix the deformed shape of the polymer film upon curing. A fine gauge wire is inserted into the epoxy prior to curing to facilitate subsequent circuit connections.

DEVICE CHARACTERIZATION

A block diagram of the testing apparatus is shown in Figure 3. The apparatus consists of a pulser (Avtech

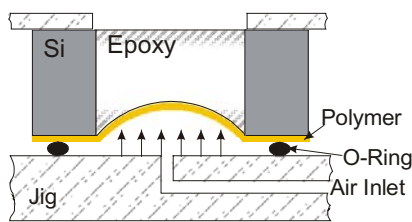


Figure 2. Schematic of pressure jig used to fabricate the ultrasonic transducers

AVB1-3-C monocyte generator, Avtech Electrosystems, Ogdensburg NY, USA) to excite the transducer, piezoelectric polymer transducer, amplification circuitry, and a digitizing oscilloscope (Agilent 54835A, Agilent Technologies, Englewood CO, USA) to observe the signal and collect data. The testing apparatus utilizes two sets of crossed diode bridges: (1) the limiter to protect the

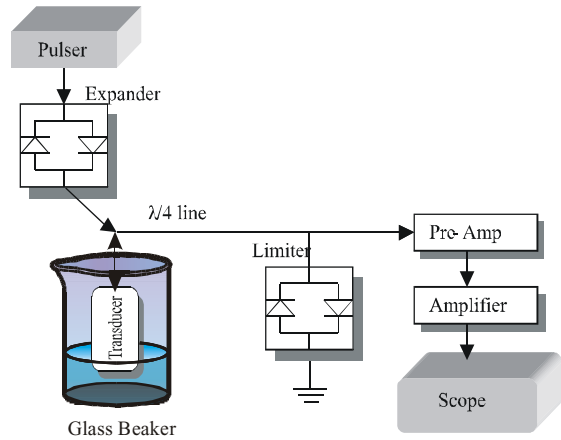


Figure 3. Diagram of test setup used to characterize the ultrasonic transducer and obtain images.

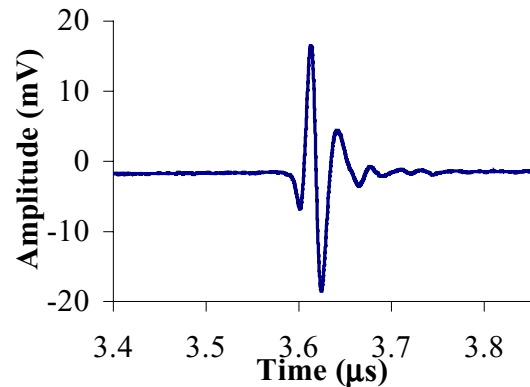


Figure 4. Pulse echo response of transducer shows minimal ringing. Time is referenced from the application of the excitation pulse.

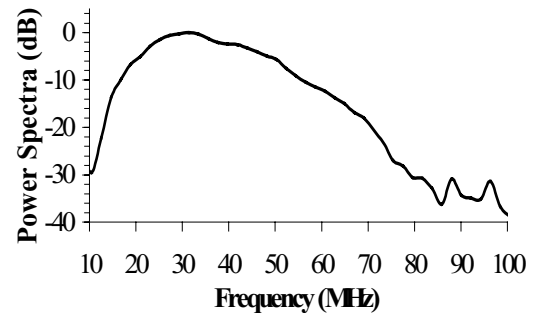


Figure 5. Pulse power spectrum of the transducer from Figure 4 showing a center frequency of ~32 MHz and a 6 dB bandwidth of ~100%.

preamplifier from the high voltage pulses ($\approx 50 V_{pp}$) and reduce the preamplifier saturation time; and (2) the expander to reduce noise contribution from the pulser by isolating it from rest of the apparatus between pulses. Transducer characterization experiments were performed using the pulse echo mode, which is the standard operational mode for ultrasonic imaging. In the pulse echo mode, the transducer emits an ultrasonic pulse and the same transducer is also used to detect the reflected pulse. Different configurations of the amplification circuitry were implemented as necessitated by the corresponding characterization experiment.

The transducers were excited by 40 MHz, 50V_{pp} monocycle pulses at a 2 kHz repetition rate in a beaker of deionized (DI) water to obtain pulse echo responses. The bottom of the glass beaker provided the reflecting surface. No amplification circuitry was used to minimize parasitic bandwidth components. A typical pulse echo response is shown in Figure 4. The pulse echo exhibits minimal ringing, which indicates a relatively large bandwidth. The corresponding power spectrum obtained via FFT of the pulse echo response is shown in Figure 5. This transducer has a center frequency of ~ 32 MHz and a 6 dB bandwidth of $\sim 100\%$. Other transducers that were fabricated using the same technique and material exhibited center frequencies of 30-45 MHz and 6 dB bandwidths of 80-110%. The variations in characteristics of the various transducers is attributed to non-uniformity in polymer film thickness and epoxy curing.

The axial responses of the transducers were characterized by exciting the transducers as described previously, but with an additional 30 dB of amplification in the circuit. The transducer was displaced relative to the bottom of the glass beaker and the peak-to-peak voltage of the corresponding pulse echo response was recorded. Figure 6 shows the results for 3 transducers with 2 mm-diameter

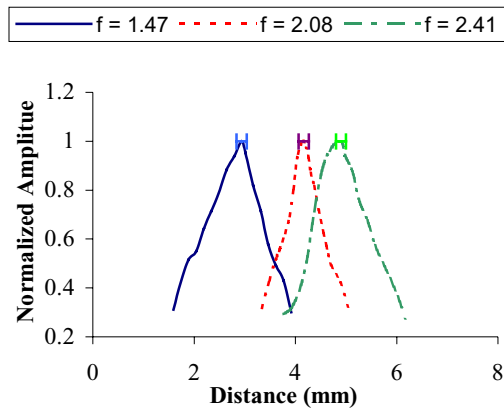


Figure 6. Normalized axial responses of transducers showing that the focal points vary with f-number. Error bars at peaks indicate the predicted focal points based upon the measured center deflections and associated error of $\pm 5 \mu\text{m}$.

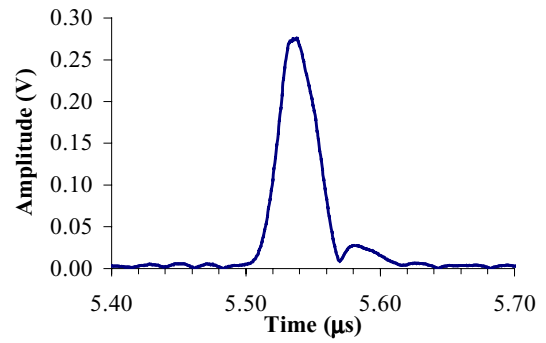


Figure 7. Hilbert transform of pulse echo response with a value of 33ns at FWHM which gives value of $50 \mu\text{m}$ axial resolution.

apertures and center deflections of 172, 123 and $102 \mu\text{m}$, respectively. These center deflections should result in f-numbers of 1.50, 2.00, and 2.45 respectively, which are in good agreement with the values of 1.47, 2.08, and 2.41, which are derived from the axial response measurements. All subsequent characterization results are presented for the transducer with the f-number of 2.08

The axial resolution of the transducer can be determined from the full-width-at-half-maximum (FWHM) of the pulse echo envelope, which is obtained via a Hilbert transform of the pulse echo response as shown in Figure 7. The FWHM has a value of 33 ns, which results in an axial resolution of $50 \mu\text{m}$, assuming sound velocity of 1500m/s in water. The lateral resolution of the transducer can be estimated from the following expression [4]:

$$\text{Resolution} = \lambda(f_{\text{number}})$$

where λ is the ultrasound wavelength relative to center frequency. The center frequency of the transducer is ~ 40 MHz, which results in a lateral resolution $\sim 38 \mu\text{m}$.

TISSUE IMAGING

Tissue is less echogenic than glass, and consequently, additional amplification is required to obtain satisfactory images. The transducer was mounted onto a PC board

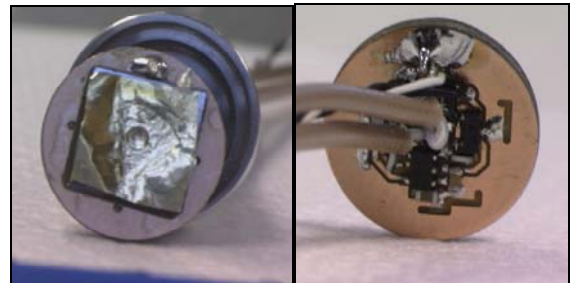


Figure 8. Front (a) and back view (b) of a transducer mounted on a printed circuit board. The transducer is the spherical shape in the center of the 1 cm-wide square die shown in (a). The backside of the PC board with the amplifier and associated biasing components is shown in (b).

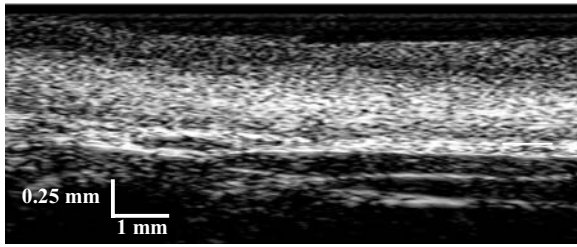


Figure 9. Image of human cadaveric aorta produced with a focused transducer. The elastin bands (horizontal lines) of the aortic tissue are clearly visible. The vertical size of the picture represents a distance of 1.5 mm while the horizontal size of the picture represents 9 mm.

incorporating a preamplifier to provide an additional 7 dB gain as shown in Figure 8. This configuration places the transducer in close physical proximity (~ 1 mm) to the preamplifier thereby eliminating ~ 4 dB of loss due to the cable. A sample of human cadaveric aorta was filleted and pinned flat onto a paraffin base. The aorta was covered with DI water and the vertical height of the transducer relative to the aorta was adjusted to obtain the maximum echo response from the tissue, thereby placing focal point of the transducer in the tissue. The transducer was then scanned using a motorized stage in one direction in increments of 0.05 mm. The reflection at each position was sampled by the oscilloscope at 1 GSa/s and saved as a file to create one scan line. This procedure was repeated for a lateral displacement of 9 mm, which generated 180 scan lines. The scan lines were subsequently compiled and standard imaging software (MATLAB, The Mathworks Inc., Natick, MA) was used to create the 256 level gray scale image of the aorta shown in Figure 9. This image clearly shows the subsurface elastin bands of the aortic tissue as well as the top and bottom surfaces. The performance of the micromachined ultrasonic transducer compare very favorably with previously published work based on conventional methods [3].

CONCLUSIONS

The design, fabrication, and characterization of novel micromachined focused ultrasonic transducers for minimally invasive medical imaging procedures has been demonstrated. Transducers were fabricated using a membrane deflection technique to produce spherical like shapes in a piezoelectric polymer film. Pulse echo responses show minimal ringing and wide bandwidths characteristics of 80-110%. Axial resolution of 50 μ m was achieved. The transducers were used to image human cadaveric aorta to reveal high-resolution subsurface structures.

ACKNOWLEDGEMENTS

The authors would like to thank Dr. Geoffrey Vince and Dr. Jim Talman of The Cleveland Clinic Foundation for helpful discussions. This work was supported by the Glennan Microsystems Initiative.

REFERENCES

- [1] S. E. Nissen and P. Yock, "Intravascular Ultrasound : Novel Pathophysiological Insights and Current Clinical Applications," *Circulation*, vol. 103, pp. 604-616, 2001.
- [2] A. Nair, B. D. Kuban, N. Obuchowski, and D. G. Vince, "Assessing spectral algorithms to predict atherosclerotic plaque composition with normalized and raw intravascular ultrasound data," *Ultrasound in Medicine and Biology*, vol. 27, pp. 1319-1331, 2001.
- [3] F. S. Foster, K. A. Harasiewicz, and M. S. Sherar, "A History of Medical and Biological Imaging with Polyvinylidene Fluoride (PVDF) Transducers," *IEEE Transactions on Ultrasonics, Ferroelectrics and Frequency Control*, vol. 47, pp. 1363-1371, 2000.
- [4] G. R. Lockwood, D. H. Turnbull, D. A. Christopher, and F. S. Foster, "Beyond 30 MHz: Applications of high frequency imaging," *IEEE Engineering in Medicine and Biology*, vol. 15, pp. 60-71, 1996.
- [5] G. R. Lockwood and C. R. Hazard, "Miniature polymer transducers for high frequency medical imaging," presented at The 1998 SPIE International Symposium on Medical Imaging, 1998.
- [6] R. G. Swartz and J. D. Plummer, "Integrated Silico-PVF₂ Acoustic Transducer Arrays," *IEEE Transactions on Electron Devices*, vol. Ed-26, pp. 1921-1931, 1979.
- [7] A. S. Fiorillo, J. V. D. Spiegel, P. E. Bloomfield, and D. Esmail-Zandi, "A P(VDF-TrFE)-based Integrated Ultrasonic Transducer," *Sensors and Actuators A*, vol. 22, pp. 719-725, 1990.
- [8] J. Mo, A. L. Robinson, D. W. Fitting, F. L. Terry, and P. L. Carson, "Micromachining for Improvement of Integrated Ultrasonic Transducer Sensitivity," *IEEE Transactions on Electron Devices*, vol. 37, 1990.
- [9] C.-H. Han and E. S. Kim, "Fabrication of Dome-Shaped Diaphragm with Circular Clamped Boundary on Silicon Substrate," presented at Twelfth IEEE International Conference on MEMS (MEMS'99), Orlando, Florida, USA, 1999.
- [10] J. Y. Pan, "A Study of Suspended-Membrane and Acoustic Techniques for the Determination of the Mechanical Properties of Thin Polymer Films," in *Electrical Engineering*. Cambridge: Massachusetts Institute of Technology, 1991.